

BTE-Barna: first-principles thermal simulation of devices based on 2D materials

M. Raya-Moreno[‡], X. Cartoixa^{*}, and J. Carrete[†]

Institut de Ciència de Materials de Barcelona (ICMAB-CSIC), Campus UAB, 08193 Bellaterra, Spain

^{*}Departament d'Enginyeria Electrònica, Universitat Autònoma de Barcelona, 08193 Bellaterra, Spain

[†]Institute of Materials Chemistry, TU Wien, A-1060 Vienna, Austria

[‡]e-mail: mraya@icmab.es

The continuous shrinking of transistors and the associated increase in integration levels, as predicted by Moore's law [1], is pushing devices to their limits, not only physically but also in terms of heat dissipation. In this context, two-dimensional materials (2DMs), thanks to their excellent properties [2] and CMOS compatibility, are promising candidates to replace silicon in transistor channels [3], [4]. Therefore, accurate simulation of thermal transport in 2DM-based devices becomes essential to optimize heat management in such devices. Despite the existence of several open-source packages [5], [6], [7] solving the problem, i.e. the Peierls-Boltzmann transport equation, informed with *ab initio* data, none of them allow for the simulation of 2DM-based systems and/or simulation beyond the relaxation approximation time (RTA) which is known to provide a very poor description of thermal properties for 2DMs [8]. In this work, we present BTE-Barna [9]—freely available at <https://github.com/sousaw/BTE-Barna>—, a software package that extends the `almaBTE` [7] package to calculate the thermal properties of devices and systems based on 2DMs and other nanosystems. Amid all new features the most relevant are:

- 1) The iterative solver has been extended to provide the effective conductivity by partially suppressing the phonon lifetimes due to boundaries [10] for the case of nanoribbons and nanowires (3D materials).
- 2) The RTA Monte Carlo simulator was updated so that now it can address finite and/or periodic 2D systems under the effect of thermal gradients and isothermal reservoirs. Moreover, it now provides information for transient

and steady-state regimes for finite systems.

- 3) A beyond-RTA Monte Carlo simulator for 2D systems has been implemented in order to provide an accurate description in those cases when the RTA falls short. This innovation, in particular, has required the implementation of a completely different Monte Carlo formalism [11] in a much more efficient way than had previously been achieved using Krylov subspace methods.

To showcase the new capabilities we have used the simulators to highlight the differences in the heat flux profile for the case of Poiseuille flow in a nanoribbon, for the case of RTA and beyond the RTA (see Figs. 1-2) as well as to compute the effective thermal flux both with MC and the iterative solver (see Fig. 3). Additionally, we also show the capabilities of our simulators to investigate hydrodynamic effects for more complex structures [12], see, for instance, vorticity and negative resistance zones in Fig. 4.

REFERENCES

- [1] G. E. Moore, *Electronics* **38**, 114117 (1965).
- [2] M. Chhowalla *et al.*, *Nat. Rev. Mater.* **1**, 16052 (2016).
- [3] D. Akinwande *et al.*, *Nat. Commun.* **5**, 5678 (2014).
- [4] J. Jiang *et al.*, *IEEE J. Electron Devices Soc.* **7**, 878-887 (2019).
- [5] A. Togo *et al.*, *Phys. Rev. B* **91**, 094306 (2015).
- [6] W. Li *et al.*, *Comput. Phys. Commun.* **185**, 1747-1758 (2014).
- [7] J. Carrete *et al.*, *Comput. Phys. Commun.* **220**, 351-362 (2017).
- [8] A. Cepelloti *et al.*, *Nat. Commun.* **6**, 6400 (2015).
- [9] M. Raya-Moreno *et al.*, *Comput. Phys. Commun.* **281**, 108504 (2022).
- [10] W. Li *et al.*, *Phys. Rev. B* **85**, 195436 (2012).
- [11] C. Landon *et al.*, *Appl. Phys.* **116**, 163502 (2014).
- [12] M. Raya-Moreno *et al.*, *Phys. Rev. B* **106**, 014308 (2022).

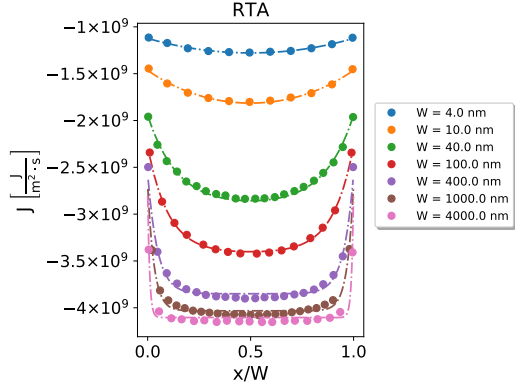


Fig. 1. Fitting to hydrodynamic equation (lines) of RTA-MC calculated heat flux (points) as a function of normalized position for phosphorene AC nanoribbons of different widths under the effect of $\nabla_{AC}T = 0.2 \text{ K nm}^{-1}$. Reproduced from Ref. [9].

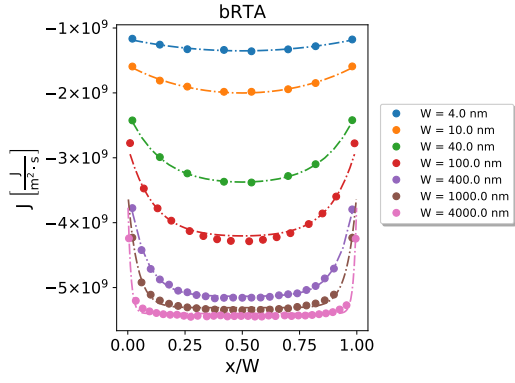


Fig. 2. Fitting to hydrodynamic equation (lines) of beyond the RTA-MC (bRTA) calculated heat flux (points) as a function of normalized position for phosphorene AC nanoribbons of different widths under the effect of $\nabla_{AC}T = 0.2 \text{ K nm}^{-1}$. Reproduced from Ref. [9].

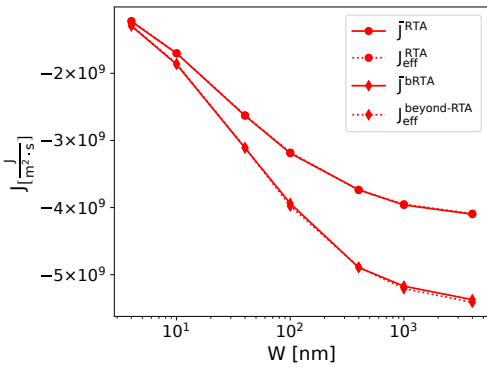


Fig. 3. Comparison between effective RTA and beyond-RTA heat fluxes for AC nanoribbons and the respective Monte Carlo obtained mean fluxes—RTA and bRTA, respectively—for a 0.2 K nm^{-1} gradient in the unbound direction. Reproduced from Ref. [9].

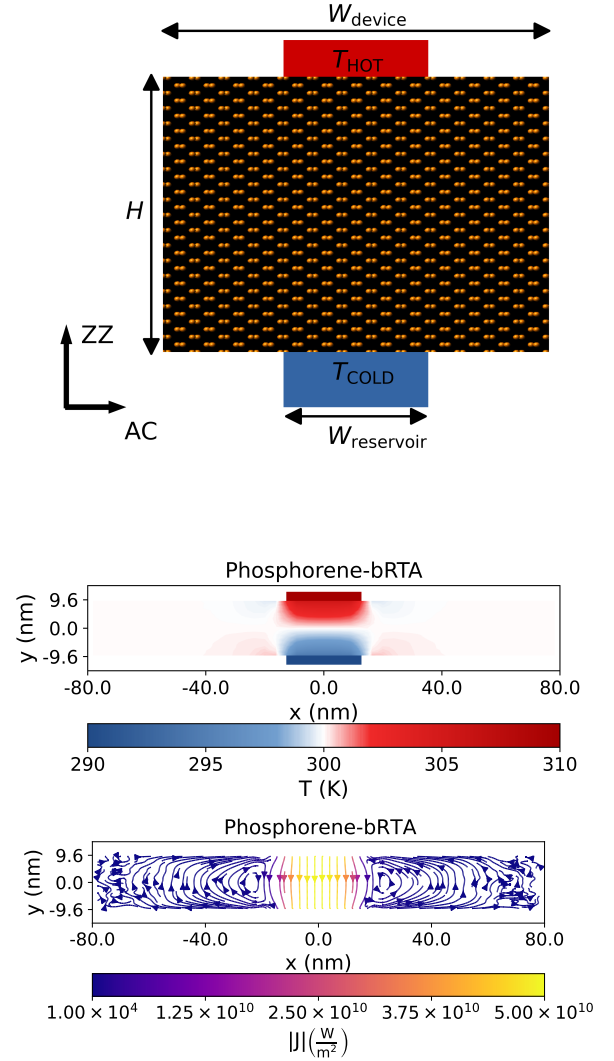


Fig. 4. Sketch of a Levitov configuration (top) with characteristic lengths H , $W_{\text{reservoir}}$ and W_{device} indicated. The transport axis, armchair (AC) and zigzag (ZZ), for phosphorene case are given as reference. The bRTA (i.e. beyond the RTA), steady-state thermal profiles (middle) and heat fluxes (bottom) illustrating vorticity for a ballistic phosphorene-based Levitov configuration with $W_{\text{reservoir}} = 25 \text{ nm}$, $W_{\text{device}} = 160 \text{ nm}$ and $H = 19.2 \text{ nm}$, $T_{\text{HOT}} = 310 \text{ K}$ and $T_{\text{COLD}} = 290 \text{ K}$. Adapted from Ref [12].